DC Scanning Field Emission Microscope Integrated with Existing Scanning Electron Microscope

Tong Wang, Charles E. Reece, and Ronald M. Sundelin

Thomas Jefferson National Accelerator Facility, Newport News, VA 23606 USA

Electron field emission (FE) from broad-area metal surfaces is known to occur at much lower electric field than predicted by Fowler-Nordheim law. Although micron or submicron particles are often observed at such enhanced field emission (EFE) sites, the strength and number of emitting sites and the causes of EFE strongly depend on surface preparation and handling, and the physical mechanism of EFE remains unknown. To systematically investigate the sources of this emission, a DC scanning field emission microscope (SFEM) has been built as an extension to an existing commercial scanning electron microscope (SEM) equipped with an energy-dispersive spectrometer (EDX/EDS) for emitter characterization. In the SFEM chamber of ultra high vacuum ($\sim 10^{-9}$ Torr), a sample is moved laterally in a raster pattern (2.5 μm step resolution) under a high voltage anode micro-tip for field emission detection and localization. The sample is then transferred under vacuum by a hermetic retractable linear transporter to the SEM chamber for individual emitter site characterization. Artificial marks on the sample surface serve as references to convert x, y coordinates of emitters in the SFEM chamber to corresponding positions in the SEM chamber with a common accuracy of ±100–200 μm in x and y. Samples designed to self-align in sample holders are used in each chamber, allowing them to retain position registration after non–*in situ* processing to

track interesting features. No components are installed inside the SEM except the sample holder, which doesn't affect the routine operation of the SEM. The apparatus is a system of low cost and maintenance and significant operational flexibility. Field emission sources from planar niobium—the material used in high-field RF superconducting cavities for particle accelerator—have been studied after different surface preparations, and significantly reduced field emitter density has been achieved by refining the preparation process based on scan results. Scans on niobium samples at ~ 140 MV/m are presented to demonstrate the performance of the apparatus.

61.16.Fk, 79.70.+q

Introduction

Enhanced field emission causes sparking problems in a wide range of high voltage vacuum devices, including vacuum switches, working in DC regime. EFE also limits the performance in the RF regime, such as in klystrons and high-field superconducting radio-frequency (SRF) resonators for particle accelerators[1 2 3]. As a source of electrons in cold cathode devices, EFE has applications in flat panel display and other microelectronic devices.

Field emission (FE) is the tunneling of electrons from metal to vacuum under high electric field, as described in the Fowler-Nordheim equation[4 5]

$$j = \frac{A \times E^2}{\phi} \times \exp(-\frac{B \times \phi^{\frac{3}{2}}}{E}) \qquad (1)$$

with $A = 1.54\times10^{-6}$, $B = 6.83\times10^{7}$, current density j in A/cm^2, electric field E in V/cm and work function ϕ in eV. According to the F-N law, no significant emission current density should be observed below the GV/m level; however, FE is encountered at much lower surface field, which is referred to as EFE and can be described to good approximation by the modified Fowler-Nordheim equation

$$I = \frac{A \times S \times \beta^2 \times E^2}{\phi} \times \exp(-B \times \frac{\phi^{\frac{3}{2}}}{\beta \times E}) \qquad (2)$$

with local field enhancement factor $\beta > 1$, effective emitting area S in cm^2 and emitting current I in A. Reviews exist on this subject[6 7] .

To study EFE, DC as well as RF apparatus have been built in several labs and show general agreement on the categories of emitters[8 9 10 11]. Advantages for DC apparatus include more accurate location of emitters and *in situ* observation and characterization of emitters. In the early 1980s, the University of Geneva was the first to set up an ultra high vacuum (UHV) DC field emission scanning apparatus, using the surface analysis system "Escalab" from Vacuum Generators, which is equipped with an electron gun, secondary electron detector and Auger analyzer for *in situ* analysis of emitters. A sample stage, anode tips and anode holder were added to the "Escalab" chamber for FE scanning. Following the example of the University of Geneva, the University of Wuppertal built a similar apparatus using "Escalab" in the early 1990s. Both produced results that show that EFE sources are localized micron or submicron sites, that many appeared to be particles or geometrical scratches/damages, and that most emitters contain foreign elements although the types of elements differ[8 9]. Some models were proposed to explain EFE, including geometrical enhancement (protrusion) model[12], metal-insulator-vacuum (MIV) model[7 13 14 15], etc. The University of Geneva FE work ended in the late 1980s, and the University of Wuppertal is focusing on diamond film and discontinuing high field work with other material. A DC scanning FE microscope (SFEM) has been built by the authors at Thomas Jefferson National Accelerator Facility (Jefferson Lab). A systematic study on various preparation techniques and handling procedures was conducted using the SFEM. A method to experimentally distinguish loosely attached foreign particles

from intrinsic material impurities was tested and used to determine the origins of emitters. Intrinsic emitters, a term that when used below will refer to grain boundary and material impurity, were suggested to be possible emitters because of the local field enhancement factor and/or evidence from early experimental work[16], but have not been experimentally confirmed or refuted for naturally occurring emitters on high purity contemporary metal surfaces. External emitters, a term that when used below will refer to geometrical damages (scratches, etc.) and foreign particles coming from handling and machining, have been evidenced by past experimental results. True F-N field emission, which occurs at above GV/m level and is sometimes also referred to as intrinsic emission, should not be confused with the intrinsic emission definition in this paper. For this work, all FE hereafter refers to EFE.

Experimental Apparatus and Procedures

Experimental Apparatus

The SFEM, as shown in Fig. 1, is a UHV device (~10^{-9} Torr), attached through a UHV bellow and gate valve to an Amray SEM 1830 with a nominal resolution of several nm. A heat treatment (HT) chamber is attached to the SFEM by a gate valve. The SFEM and HT chambers each have a dedicated ion pump and use the turbo and mechanical pumps of the SEM system for roughing. Samples are loaded via the SEM, and can be transferred under vacuum to the other two chambers by a hermetic retractable linear transporter. The SFEM

and HT chambers are supported by a vibration-isolated frame. The UHV bellow between the SFEM and SEM provides vibration isolation between the two chambers.

Fig. 1 Experimental apparatus (top view).

Within the SFEM chamber, samples of slightly larger than 25 mm diameter can be moved in x, y, and z under an anode tip by a motorized high precision sample manipulator (from Vacuum Generators). Anode tips are mounted on an anode holder that can be moved linearly for tip exchange. Tungsten anodes of 150, 10 and 1 μm tip curvature radius can be selected for coarse, medium and fine scans. The resolution of sample manipulation in x, y, and z is 2.5 μm, and the travel range in the x, y plane is a circle of 25 mm diameter determined by the size of the UHV bellow (35 mm inner diameter) employed in the manipulator and the size of the sample probe (10 mm diameter). A circular travel limit device of 35 mm inner diameter was designed by the authors and installed inside the chamber concentric to the mounting flange of the UHV bellow of the sample manipulator, as illustrated in Fig. 2. The top stainless steel ring of the device is insulated from the rest of the device and the chamber by ceramic, and connected to the "limit switch" signal (+5 V) on the stepper motor controller card. When the sample probe (at ground potential) travels to the limit and touches the top ring, the limit switch is then closed and the signal can be detected by the computer through the controller card. This design avoids potential damage to the manipulator in case of overdrive and enables full utilization of its travel range, thus providing a larger scan area than other DC FE scanning apparatus built by the University of Geneva (12 mm × 12 mm) and by the University of Wuppertal (15 mm dia.).

Fig. 2 Illustration of sample circular travel limit switch

A long distance optical microscope is mounted above a viewport on the SFEM chamber for observation of the scanning process and emitting sites through a CCD camera and a TV monitor. The long distance microscope from Questar has a nominal resolution of 1.1 μm at a working distance of 15 cm.

The sample and sample holders in three chambers are specially designed for the sample to have self-alignment capability, i.e. the sample can return to its previous location and orientation after non–*in situ* processing. The repeatability in x, y is ~±140 μm. With the additional aid of surrounding grain shapes as seen with the SEM, interesting micron and submicron features can be tracked through non–*in situ* as well as *in situ* preparation. Similarly, the emitting behavior of individual emission sites can also be tracked. Samples slightly larger than 25 mm diameter are used so that the edge area that is vulnerable to machining damage can be avoided during FE scan. To illustrate the capability of the design to facilitate the relocation of micron to submicron features (and also a way to experimentally distinguish external particles from material impurities), pictures of a foreign microparticle before and after water rinse are shown in Fig. 3.

Fig. 3 The methodology to distinguish external particles from material impurities. A foreign microparticle is shown before and after ultrasonic water rinse.

After emitters are located in the SFEM chamber, the sample is transferred to the SEM chamber for emitter characterization. The SEM is equipped with EDS capable of windowless operation for light element sensitivity. Three artificial marks on each sample

surface are used as fiducials to transfer x, y coordinates of emitters in the SFEM chamber to those in the SEM chamber. The common accuracy in locating emitters under SEM is ±100–200 μm. As the sample preparation process is progressively refined and controlled, the number of emitters per sample has dropped to 1–2/sample, as addressed below. With the low number of emitters, and the fact that the ±500 μm area around the calculated emitter location is always closely examined for any features under the SEM at 320× magnification, the identification of emitters is routinely unambiguous, and can often be further confirmed by a second FE scan after an ultrasonic water rinse to remove the suspected emitting particle.

The HT chamber is designed for the purpose of sample outgassing by external radiation and sample thermal processing by electron bombardment up to 1400°C. The temperature can be monitored by an optical pyrometer.

The SFEM apparatus is located in a Class 1000 cleanroom to reduce risk of contamination during sample handling.

Experimental circuit and procedures

The experimental measurement and control circuit is illustrated in Fig. 4. The high voltage power supply is controlled by a PC to output a voltage ramp from 0 to 40 kV, or until a current threshold is reached, usually 1–2 nA detected by a picoammeter. The 100 GΩ current limiting resistor is specially made to be UHV compatible and is mounted

inside the FE chamber to reduce the ability of the energy stored in the cable capacitance to damage or destroy emitters during a vacuum arc. The entire scan process, including 3-axis sample motion automation and instrument control, data acquisition and analysis, and image acquisition, is performed by programs written in LabView™.

Fig. 4 Experimental circuit diagram

The gap between anode tip and sample (usually set at 100–200 μm) during each scan is maintained by adjusting the sample position in z while moving in x, y according to the mean surface plane. The mean surface plane is obtained by fitting multi-point profile data for each sample surface. For a planar sample, usually five to nine points dispersed over the surface area are sufficient to produce a good approximation. The profile data are obtained by moving the sample up in z until it slightly touches the anode tip at the selected points, indicated by a short circuit between sample and anode tip. This method results in a gap consistency of about ±10 μm determined from the long distance optical microscope. An option in this profiling step is to raise the sample until in focus as viewed from the top from the optical microscope while maintaining the parameters of the microscope. The gap consistency is compromised due to the depth of field of the microscope (~ 20 μm at current working distance), but this method leaves an untouched surface. An illustrative interpolation and extrapolation of the multi-point profile is shown in Fig. 5.

Fig. 5 Illustrative interpolation and extrapolation of nine-point profile data to 25mm × 25 mm area. ("+": profile points)

The FE scan on an entire surface can be done using anode of 150 or 10 μm tip radius for coarse to medium resolution scan. The electric field is dependent on anode shape, tip radius and gap distance. The electric field correction factor κ (= V/Ed) is calculated based on Ph. Niedermann's analysis[8], with V as the applied anode voltage, d as the gap distance from anode apex to cathode plane, and E as the electric field at cathode directly below anode tip. For various anode and gap configuration in our experiment, κ is calculated to range from 1.34 to 3. After emitters are located, a local fine scan around the emission sites using a needle of 1 μm tip radius at a gap of 50 μm will follow to accurately locate the emission center. See Fig.6 for an illustrative plot of scan data, namely $y+C(V_0-V(x, y))$ versus x. V_0 is the maximum output voltage of the power supply, $V(x, y)$ is the highest voltage reached at (x, y) before the threshold current is exceeded, and C is an adjustment factor to accommodate data display. The local scan data is plotted at the right.

Fig. 6 Illustration of coarse scan at entire sample surface (ϕ25 mm) at 140 MV/m using anode of 150 μm tip curvature radius (left), along with local scan of 100 μm × 100 μm area at the center of the outlined emitter using anode of 1 μm tip curvature radius (right).

The gap can be calibrated at the emitter by centering the anode at the emission center and gradually reducing the gap while adjusting the high voltage to maintain a constant current. The extrapolation of V versus gap plot to $V = 0$ is set as gap = 0. The slope of the linear fitting line divided by the correction factor κ gives the calibrated electric field, as shown in Fig. 7.

Fig. 7 Calibration of gap and electric field at emitting site

To characterize an individual emitter, the field enhancement factor β and effective emitting area S can be obtained by linear fitting of $\ln(I)/E^2$ versus $1/E$. (Refer to Equation (2).)

Experimental results

The present EFE study is made on bulk niobium (Nb) surfaces such as is used in SRF resonating cavities employed in particle accelerators. In the same manner as is done with Nb cavities, a number of Nb samples made from high purity (RRR~300) Nb sheet were chemical etched by BCP (buffered chemical polish, HF (49%):HNO_3 (69%):H_3PO_4 (85%) = 1:1:1) to remove machining damage[1]. To remove acid residue and particles introduced during handling, ultrasonic cleaning in de-ionized water is performed immediately following BCP. Early tests by the authors had shown 8–60 emitters/sample at 70 or 140 MV/m, but improvement in the machining and handling process has lowered the number to 3–8/sample[17]. After making samples slightly larger to avoid scanning the edge area (which is prone to machine damage), and after replacing the previous 1 GΩ current-limiting resistor with the present 100 GΩ, more tests were run. The results are shown in Table 1.

Table 1: Results from BCP prepared samples at ~ 140 MV/m. #75 BCP-1, 2 are after 250, 300 μm BCP removal respectively on sample #75; #72 BCP-1, 2 are after 250, 300 μm BCP removal respectively on sample #72; #76 BCP-1 is after 250 μm BCP removal on sample #76.

	#75 BCP-1	#75 BCP-2	#72 BCP-1	#72 BCP-2	#76 BCP-1
Foreign particles	1	2	0	0	0
Emitters destroyed by vacuum arc	0	0	1	1	1

As illustrated in Table 1, further reduced occurrence of FE has been achieved on a number of Nb samples at ~140 MV/m. Currently observed emitters can be divided into two categories: foreign particles and emitters destroyed by vacuum arc. Foreign particles are categorized as such because of their appearance and/or the fact that they are rinsed away by a second water rinse in ultrasonic as observed under SEM. (Refer to Fig. 3.) The foreign particles listed in Table 1 emit at electric field from 35 to 100 MV/m. SEM pictures of some of the typical particulate emitters are shown in Fig. 8.

Fig. 8 A selection of SEM pictures of typical foreign particulate emitter. (Both emitters shown contain Nb, Fe, Cr.)

As shown in Table 1, not only foreign particles, but also the occurrence of vacuum arcs are furtner reduced compared to previously reported results by the authors[17]. Vacuum arcs or sparks—transient vacuum breakdown within the gap—are observed via the optical microscope. The mechanisms that initiate vacuum arcs are very complex. Many

theories for cathode-initiated breakdown are based on the initial heating of emitters to reach thermal instability, which is unlikely for intrinsic emitters because of the good thermal contact with the bulk material. Secondly, the transfer of weakly bound microparticles from cathode to anode, or vice versa due to pure mechanical forces from strong electric field, has been experimentally proved to be able to cause field emission and breakdown[7]. Some particles caused vacuum arc but weren't completely destroyed, and therefore could be identified as foreign particles in the same way as described above. Furthermore, the fact that the average number of vacuum arcs per sample can be furtner reduced to less than 1/4 of the previously reported value[17] also strengthens the authors' view that they are less likely caused by intrinsic emitters, which should largely remain unchanged in number, since all the samples were cut from the same Nb sheet.

From the results presented above, the following conclusions are drawn:

- Undestroyed emitting sites are found to be foreign microparticles.
- No evidence of intrinsic emitters is observed up to 140 MV/m, although more samples need to be studied for better statistics.
- Further reduction in FE for Nb samples and presumably SRF cavities can be achieved by improving material preparation techniques and more stringent particulate control.

Discussion

The apparatus has been used to conduct over 50 FE scans (total scan area: ~250 cm^2) and characterizations and has worked reliably and consistently. The system can be used to

refine new as well as existing surface treatment techniques, handling procedures and storage methods before being applied to Nb cavities or other devices. Thin films and other processes that are being developed and intended for SRF application or DC high voltage vacuum insulation—for instance, laser or electron beam processed material—can also be evaluated by the apparatus for FE characterization. Other potential uses for the system include examination of material relevant to field emission displays.

Acknowledgment

The authors would like to thank Larry Phillips for his help with the apparatus, Brett Lewis and Tom Goodman for their assistance with the maintenance of the SEM and Steve Corneliussen for his careful review.

* This work was supported by the U.S. DOE Contract No. DE-AC05-84ER40150.

List of tables

List of Figure Captions

[1] H. Padamsee, J. Knobloch, and T. Hays, *RF Superconductivity for Accelerators* (Wiley and Sons, New York, 1998).

[2] Proc. of the 7th Workshop on RF Superconductivity, CE Saclay, Gif sur Yvette, France, (1995), edited by B. Bonin

[3] Proc. of the 8th Workshop on RF Superconductivity, Padova, Italy, (1997).

[4] R. H. Fowler and L. Nordheim, Proc. Roy. Soc. London A 119, 173, (1928).

[5] L. Nordheim, Proc. Roy. Soc. London A 121, 626, (1928).

[6] R. J. Noer, Appl. Phys. A **28**, 1, (1982).

[7] R. V. Latham, *High Voltage Vacuum Insulation* (Academic Press, London, 1981)

[8] Ph. Niedermann, Ph. D thesis, University of Geneva, 1986.

[9] E. Mahner, G. Muller, H. Piel, and N. Pupeter, J. Vac. Sci. Technol. B **13 (2)**, 607, (1995).

[10] J. Tan, Proc. of the 7th Workshop on RF Superconductivity, CEA/Saclay, 105, (1995), edited by B. Bonin

[11] D. Moffat, P. Barnes, T. Flynn, J. Graber, L. Hand, W. Hartung, T. Hayes, J. Kirchgessner, J. Knobloch, R. Noer, H. Padamsee, D. Rubin, and J. Sears, Proc. of the 5th Workshop on RF Superconductivity, DESY, 245, (1991).

[12] H. H. Race, General Electric Review, 43, 365, (1940).

[13] R. V. Latham, Vacuum **32**, 137, (1982).

[14] C. S. Athwal and R. V. Latham, J. Phys. D: Appl. Phys. **17**, 1029, (1984).

[15] C. S. Athwal and R. V. Latham, Physica C **104**, 189, (1981).

[16] B. M. Cox, J. Phys. D: Appl. Phys. **8**, 2065, (1975).

[17] T. Wang, C. E. Reece, and R. M. Sundelin, Proc. of the 10th Workshop on RF Superconductivity, Tsukuba City, Japan, (2001) to be published.

Fig. 1 Experimental apparatus (top view).

Tong Wang at al. Review of Scientific Instruments

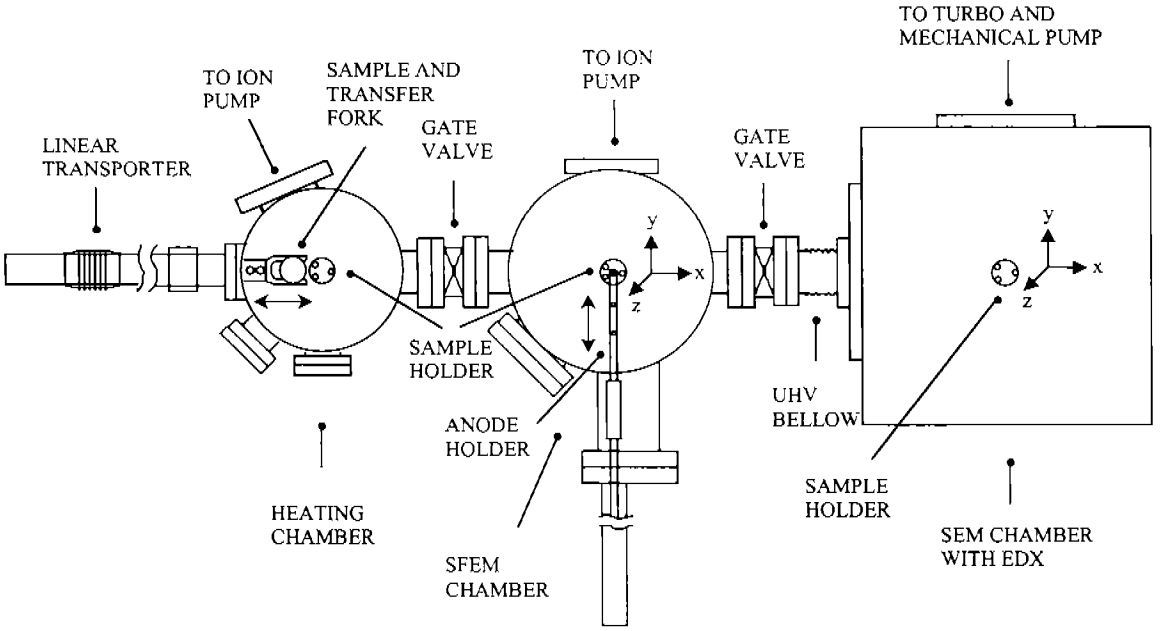

Fig. 2 Illustration of sample circular travel limit switch

Tong Wang et al. Review of Scientific Instruments

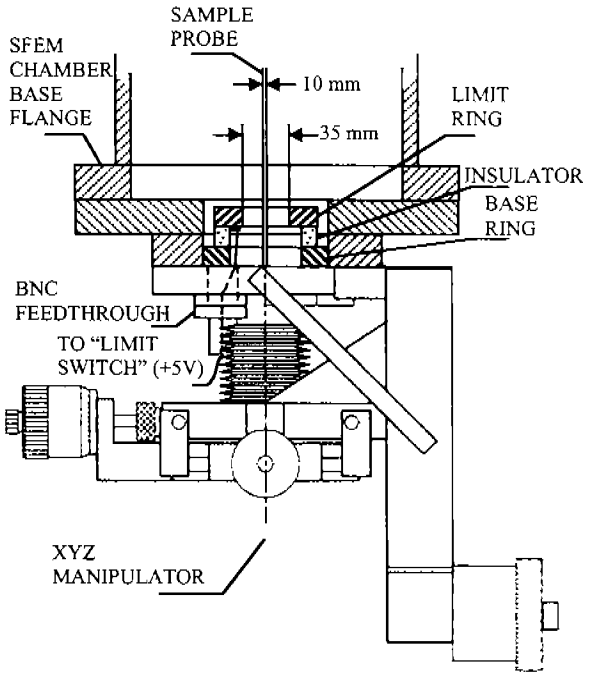

Fig. 3 The methodology to distinguish external particles from material impurities. A foreign microparticle is shown before and after ultrasonic water rinse.

Tong Wang et al. Review of Scientific Instruments

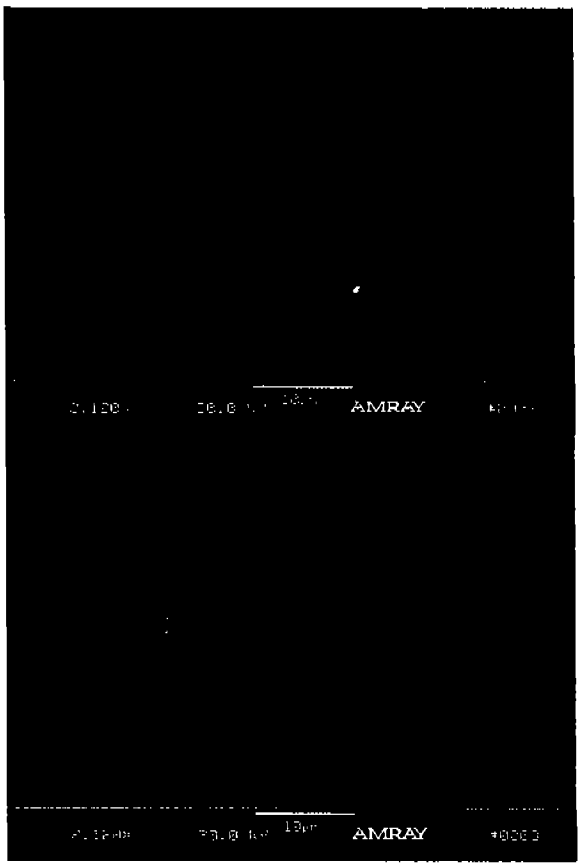

Fig. 4 Experimental circuit diagram

T. Wang, et al. Review of Scientific Instruments

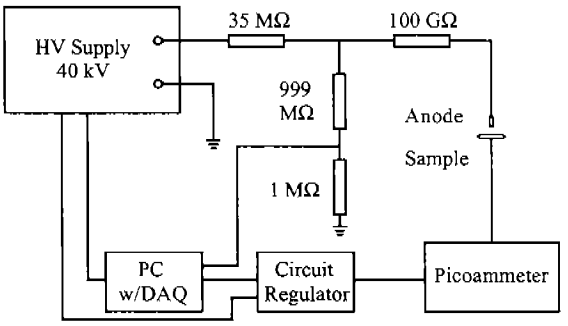

Fig. 5 Illustrative interpolation and extrapolation of nine-point profile data to 25 mm x 25 mm area. ("+": profile points).

Tong Wang et al. Review of Scientific Instruments

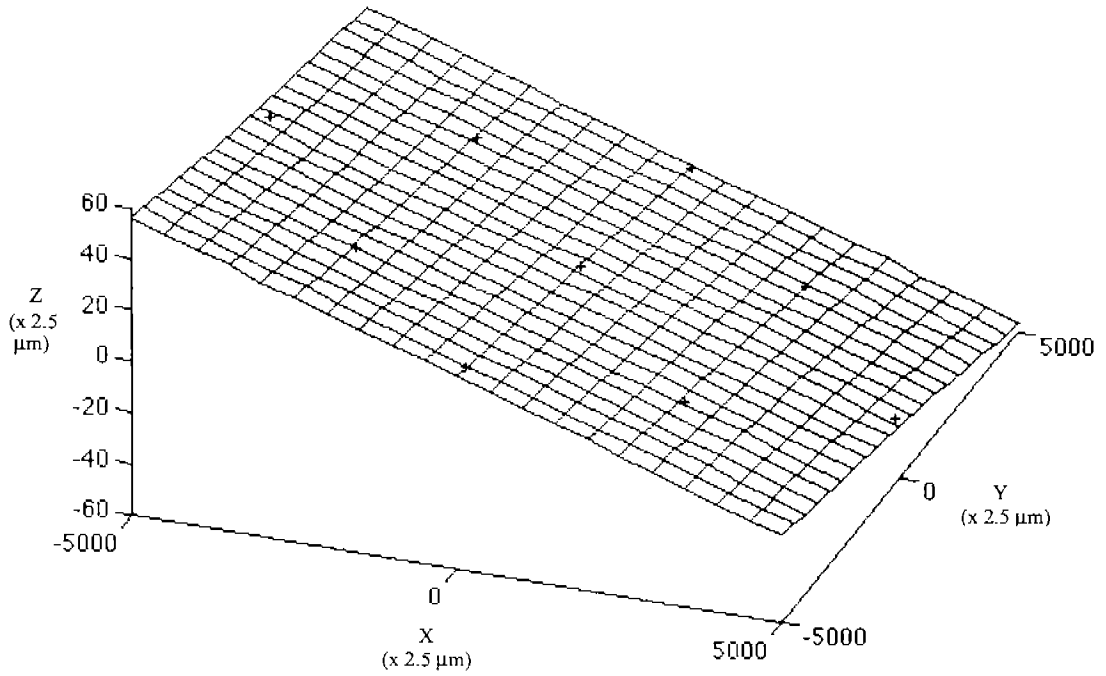

Fig. 6 Illustration of coarse scan at entire sample surface (ϕ25mm) at 140 MV/m using anode of 150 μm tip curvature radius (left), along with local scan of 100 μm × 100 μm area at the center of the outlined emitter using anode of 1 μm tip curvature radius (right).

Tong Wang et al. Review of Scientific Instruments

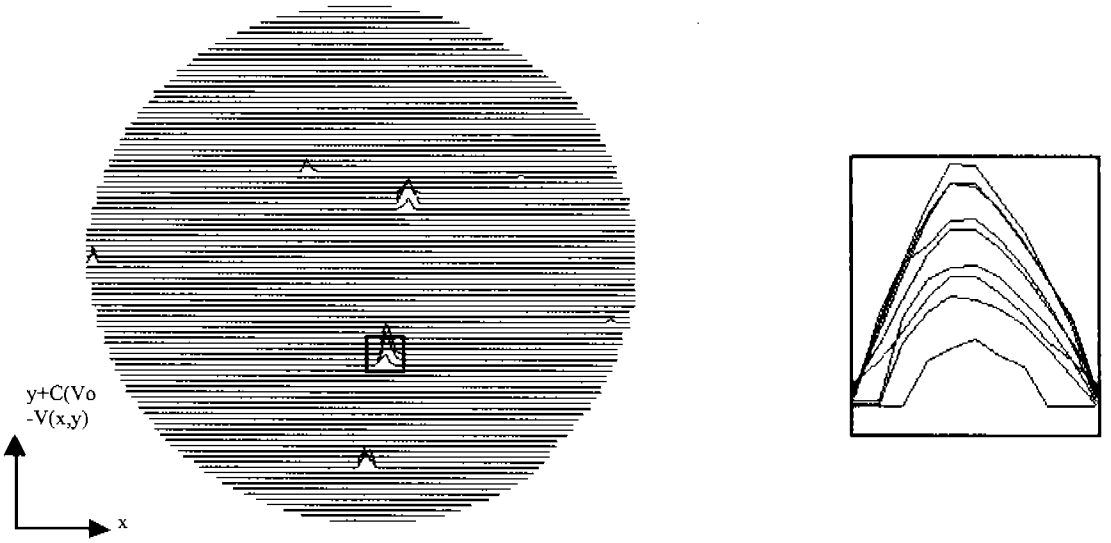

Fig. 7 Calibration of gap and electric field at emitting site

Tong Wang, et al. Review of Scientific Instruments

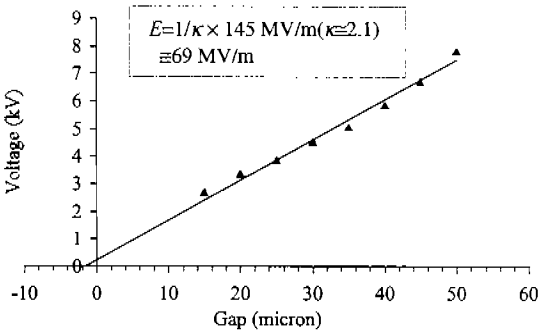

Fig. 8 A selection of SEM pictures of typical foreign particulate emitter. (Both emitters shown contain Nb, Fe, Cr.)

Tong Wang, et al. Review of Scientific Instruments